Interactions Between Madden Julian Oscillation (MJO) Variability and Equatorial Waves

MIDN 1/C Michael Magee[1], Gina Henderson[1], Scott Hottovy[2]

[1]Dept of Ocean and Atmospheric Sciences, U.S. Naval Academy (USNA); [2]Mathematics Dept, USNA

INTRODUCTION

The Madden Julian Oscillation (MJO) is the dominant mode of tropical intraseasonal variability, with a period of roughly 30–90 days (Wheeler and Kiladis 1999; Wheeler and Hendon 2004). Physically, the MJO is a system of tropical convection that propagates about the equator in an eastward direction. The MJO has two components, the first being a large vertical column of enhanced rainfall (convective column), and the second being the vertical columns of suppressed rainfall on either side of the central column (Figure 1). Due to its size and scale, the MJO acts as the primary driver of precipitation in the tropical latitudes, and bridges the gap between local weather patterns and large scale climate patterns across the globe.

Equatorial Waves (EWs) are propagating disturbances, with periods of a few days to several weeks, that are "trapped" between the tropical latitudes of the Earth. They appear as oscillations in field variables, such as temperature, pressure, and flow, with magnitudes large enough to probe changes in weather (Wheeler 2003).

The Problem: Through interactions with EWs, the MJO is able to influence weather across the globe. Understanding these interactions is crucial to increasing our ability to predict global weather.

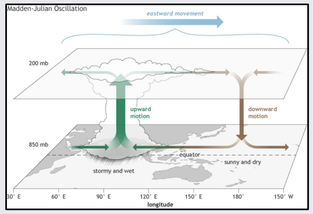


Figure 1. *The physical structure of the Madden-Julian Oscillation (MJO). A column of enhanced convection flanked by columns of suppressed convection (only one shown). The MJO typically spans vertically from 850mb (~1500m) to 200mb (~12000m). The whole system is propagating eastward across the equator (Gottschalck 2014).*

RESEARCH OBJECTIVES

1. How does changing MJO amplitude/strength impact the interactions with equatorial waves?
2. How does changing MJO seasonality and geographic phase impact the interactions with equatorial waves?
3. How does MJO variability impact the physical structure of equatorial waves and the atmosphere at large?

METHODS

Wavenumber Frequency Power Spectra: This project combines two widely used tools in MJO literature. This power spectra, visualizes the wavenumbers and frequencies for equatorial waves (EWs) and the MJO, as well as their associated power (Wheeler and Kiladis 1999).

RMM Index: The RMM Index utilizes 200mb winds, 850mb winds, and OLR to create an index that quantifies the location (phase) and strength of the MJO (Wheeler and Hendon 2004).

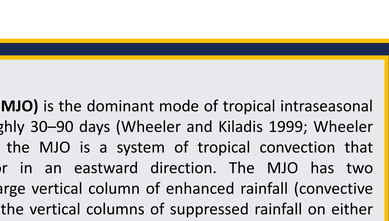


Figure 2. *Symmetric OLR (SOLR) power spectra (a), and antisymmetric OLR (AOLR) power spectra (b), with colors showing the spectral power for the MJO, Kelvin wave, and ER wave (a), and MRG wave (b). MJO RMM index (c) shows the amplitude and location of the MJO at a each day within our data set (1975-2014). By combining the power spectra and RMM index, we isolate different MJO parameters to visualize the effects on equatorial waves (EWs).*

Our Data: We used global daily OLR, tropical daily 200mb zonal wind, and tropical daily 850mb zonal wind. This data was provided by the NOAA PSL, in Boulder, Colorado, and covers 40 years, from 1975 to 2014. All the data was confined to the tropical latitudes of 15°N to 15°S.

Our Method: To investigate our three objectives:

- Recreate the power spectra and the RMM index, using our daily OLR and wind data, and combine these two tools (Figure 2).
- Segment the OLR data into different MJO amplitudes, phases, and seasons, and create power spectra
- Compare and analyze against the all data power spectra, to quantify the interactions between MJO variability and EWs.

OBJECTIVE 1: MJO AMPLITUDE

In order to isolate the MJO amplitude parameter, we utilized our Wheeler and Hendon RMM index to segment our data based on various MJO amplitude limits. An active MJO has been defined as having an amplitude greater than 1.0 on the RMM index (Wheeler and Hendon 2004). Thus, any amplitude less than 1.0 represents a weak, inactive MJO, and any amplitude greater than 1.0 represents an active MJO. We defined 5 different amplitude limits: MJO amplitudes < 1.0, > 1.0, > 1.5, > 2.0, > 2.5. These limits were chosen in order to capture the difference between an inactive MJO and an active MJO, over a broad range of active thresholds. We created a wavenumber frequency power spectra for each segmented amplitude, and subtracted out the all data power spectra to analyze the percent difference between the two (Figure 3). This poster focuses on the results from an MJO amplitude less than 1, and an MJO amplitude greater than 2.5 (Figure 4).

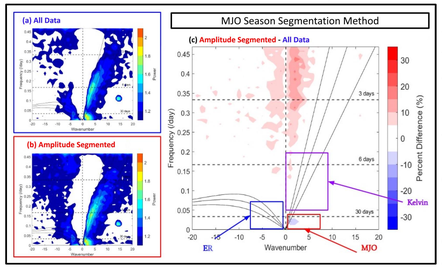


Figure 3. *Total data spectra (symmetric only) (a) and amplitude segmented spectra for the MJO amplitude of interest (b). By subtracting the total data spectra from the amplitude segmented spectra, and dividing it by the total data spectra, plot (c) is produced. Plot (c) shows the percentage difference of signal strength due to the amplitude of interest compared to the average behavior. Red colors indicate signals that are stronger than the total data, while blue colors indicate signals that are weaker than the total data. The shallow water dispersion curves for Kelvin waves and Equatorial Rossby waves are plotted as solid black lines.*

MJO Amplitude < 1.0:

The SOLR spectra demonstrates that there is no enhanced, or weakened signal for either the Kelvin wave or ER wave, indicating that inactive MJO occurrences have no influence on symmetric EW activity (Figure 5(a)). The AOLR spectra demonstrates the same conclusion for MRG waves (Figure 5(b)).

MJO Amplitude > 2.5:

The SOLR spectra demonstrates that the range of wavenumbers within the enhanced MJO envelope has increased, spanning from a wavenumber of 1 to around 6 (Figure 5(c)). There are several enhanced signals for the ER wave, ranging as high as 15-20% (Figure 5(c)). Therefore, extreme strengths of MJO have a substantial influence on ER wave activity. Interestingly, there are no substantial signals along the Kelvin dispersion (Figure 5(c)). The AOLR spectra demonstrates that westward MRG (negative wavenumbers) are now much weaker, showing signals about 10-20% weaker (Figure 5(d)). Interestingly, eastward MRG signals are stronger, with signals that are 10-15% stronger (Figure 5(d)).

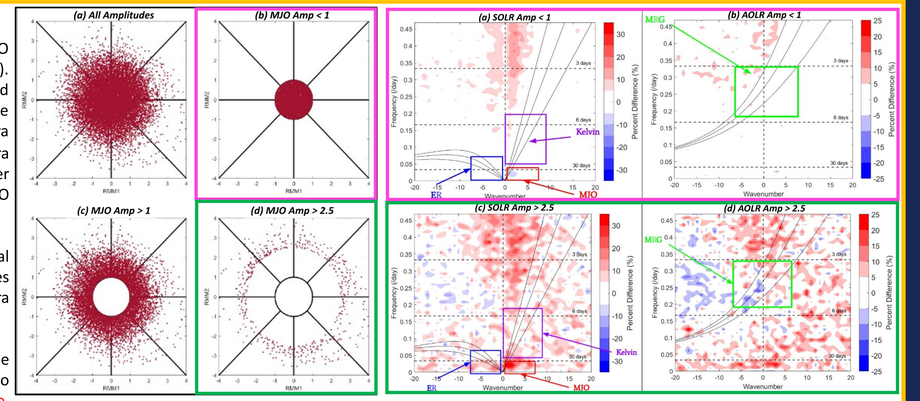


Figure 4. (Left) *Four different versions of our Wheeler and Hendon RMM index are shown, to visualize the MJO amplitude segmentation process. Plot (a) shows all MJO amplitudes. Plot (b) shows only MJO amplitudes less than 1. Plot (c) shows MJO amplitudes greater than 1. Plot (d) shows MJO amplitudes greater than 2.5. The pink and green boxes over plot (b) and (d) respectively identify the two amplitudes presented on this poster.*

Figure 5. (Right) *The symmetric OLR (SOLR) spectra are shown for MJO amplitudes of (a) less than 1, and (c) greater than 2.5. The antisymmetric OLR (AOLR) spectra are shown for MJO amplitudes of (b) less than 1, and (d) greater than 2.5. The pink and green boxes identify which RMM index from Figure 4 produced the spectra in Figure 5. Each plot was made in accordance with Figure 3 (c). In plots (a) and (c), The shallow water dispersion curves for Kelvin waves and Equatorial Rossby waves are plotted as solid black lines. Colored boxes provide a visual locator for the two waves, as well as the MJO. In plots (b) and (d), The shallow water dispersion curves for Mixed Rossby Gravity waves are plotted as solid black lines. A green colored box provides a visual locator for the wave.*

OBJECTIVE 2A: MJO SEASON

In order to isolate the MJO season parameter, we segmented our data based on four different 3 month season limits, for Winter, Spring, Summer, and Fall. Our segments were created by capturing the 9 months of OLR data outside of the desired season, creating a wavenumber frequency power spectra, then subtracting the 9 month spectra from the total data spectra (Figure 6). This segmentation method was used to maximize the number of segments available, in an effort to reduce noise.

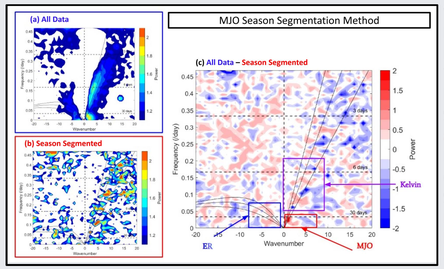


Figure 6. *Total data spectra (symmetric only) (a) and season segmented spectra for the 9 months of the year besides the season of interest (b). By subtracting the 9 month segmented spectra from the total data, plot (c) is produced, which shows the signal difference during the season of interest, compared to the total data. Red colors indicate signals that are stronger than the total data, while blue colors indicate signals that are weaker than the total data. The shallow water dispersion curves for Kelvin waves and Equatorial Rossby waves are plotted as solid black lines.*

Winter: The MJO signal is stronger in the Winter season. The ER and Kelvin signals show some enhancement as well, though noise makes it hard to deduce a strong relationship (Figure 7(a)). East and west MRG signals are stronger, however some higher frequency east MRG signals are weakened (Figure 8(a)).

Spring: The MJO signal is stronger in the Spring season. Kelvin and ER signals are both weaker during the Spring (Figure 7(b)). East and west MRG signals are both stronger in the Spring (Figure 8(b)).

Summer: The MJO signal is weaker in the Summer season. Kelvin signals are weaker, while ER signals are weaker, at higher wavenumbers (Figure 7(c)). East MRG signals are weaker at higher frequencies, while west MRG signals are unchanged (Figure 8(c)).

Fall: The MJO signal is much weaker in the Fall season. Kelvin signals are stronger at low frequencies and weaker at high frequencies, while ER signals are weaker (Figure 7(d)). West MRG signals are much weaker, while east MRG signals are weaker at higher frequencies, but stronger at lower frequency (Figure 8(d)).

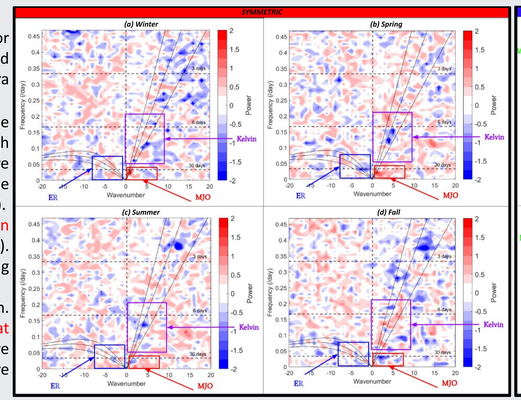


Figure 7. (Left) *The symmetric OLR (SOLR) spectra are shown for all four seasons, (a) Winter, (b) Spring, (c) Summer, and (d) Fall. Winter covers the months of December, January, and February (DJF). Spring covers the months of March, April, and May (MAM). Summer covers the months of June, July, and August (JJA). Fall covers the months of September, October, and November (SON). Each plot was made in accordance with Figure 6 (c). The shallow water dispersion curves for Kelvin waves and Equatorial Rossby waves are plotted as solid black lines. Colored boxes provide a visual locator for the two waves, as well as the MJO.*

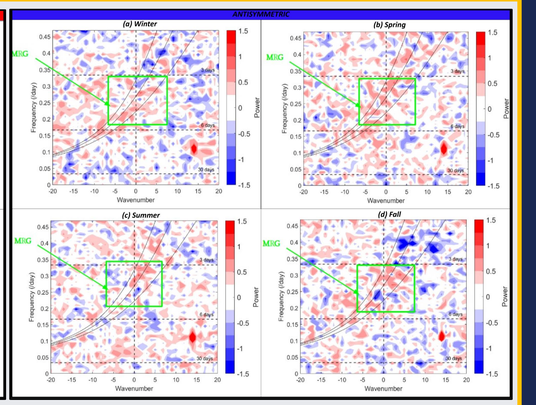


Figure 8. (Right) *As in Figure 7 for the antisymmetric OLR (AOLR). The shallow water dispersion curves for Mixed Rossby Gravity waves are plotted as solid black lines. A green colored box provides a visual locator for the wave.*

FUTURE WORK

1. **Noise reduction.** We will continue to work on methods that will reduce the noise in our figures, especially the seasonal plots. We have tried several modifications already, to include adjusting segment overlap/size, colormaps, and various segment methods.
2. **Objective 2B: MJO phase.** We will analyze the effects of MJO on EW interactions at all 8 defined geographic phases on the RMM Index. This method will follow the methodology of objectives 1 and 2A.
3. **Objective 3: Physical structure.** We will analyze the effects of MJO variability on the physical structure of EWs. By mapping our previous results onto characteristic wave modes, we will visualize how the physical structure of EWs are impacted by MJO variability.

REFERENCES

Gottschalck, J., 2014: What is the MJO, and why do we care?. NOAA, Accessed 10 November 2023, https://www.climate.gov/news-features/blogs/enso/what-mjo-and-why-do-we-care.

Wheeler, M. C., 2003: TROPICAL METEOROLOGY | Equatorial Waves. *Encyclopedia of Atmos. Sci.*, **1**, 2313-2325, https://doi.org/10.1016/B0-12-227090-8/00414-0.

Wheeler, M. C., and H. H. Hendon, 2004: An All-Season Real-Time Multivariate MJO Index: Development of an Index for Monitoring and Prediction. *Mon. Wea. Rev.*, **132**, 1917–1932, https://doi.org/10.1175/1520-0493(2004)132<1917:AARMMI>2.0.CO;2.

Wheeler, M., and G. N. Kiladis, 1999: Convectively Coupled Equatorial Waves: Analysis of Clouds and Temperature in the Wavenumber–Frequency Domain. *J. Atmos. Sci.*, **56**, 374–399, https://doi.org/10.1175/1520-0469(1999)056<0374:CCEWAO>2.0.CO;2.

ACKNOWLEDGEMENTS

This research is funded by the Office of Naval Research (ONR) with grant number **N0001423WX00746.** This project is part of the Trident Scholar program at the United States Naval Academy (USNA). Thank you to MSC at USNA for printing this poster.